


Design, synthesis, and biological evaluation of histone deacetylase inhibitor with novel salicylamide zinc binding group

Ji Hyun Kim, MS, Khan Hashim Ali, MS, Yong Jin Oh, PhD, Young Ho Seo, PhD* 

Abstract

Introduction: Histone deacetylases (HDACs) have emerged as important therapeutic targets for various diseases, such as cancer and neurological disorders. Although a majority of HDAC inhibitors use hydroxamic acids as zinc binding groups, hydroxamic acid zinc-binding groups suffer from poor bioavailability and nonspecific metal-binding properties, necessitating a new zinc-binding group. Salicylic acid and its derivatives, well-known for their therapeutic value, have also been reported to chelate zinc ions in a bidentate fashion. This drew our attention towards replacing hydroxamic acid with salicylamide as a zinc-binding group.

Methods: In this study, for the first time, compound 5 possessing a novel salicylamide zinc-binding group was synthesized and evaluated biologically for its ability to inhibit various HDAC isoforms and induce acetylation upon α -tubulin and histone H3 among MDA-MB-231 cells.

Results: Compound 5 exhibits selective inhibition against class I HDAC isoforms (HDAC1, 2, and 3) over class II and IV HDAC isoforms (HDAC4, 6, and 11). The exposure of MDA-MB-231 cells to compound 5 efficiently induced the acetylation of more histone H3 than α -tubulin, suggesting that compound 5 is a class I selective HDAC inhibitor. Moreover, the molecular docking study indicated that the salicylamide zinc-binding group of compound 5 coordinates the active zinc ion of class I HDAC2 in a bidentate fashion.

Conclusion: Overall, salicylamide represents a novel zinc-binding group for the development of class I selective HDAC inhibitors.

Graphical abstract: (<http://links.lww.com/MD/G668>)

Abbreviations: δ = parts per million, Boc₂O = di-tert-butyl dicarbonate, C = O = Carbonyl group, DIPEA = N,N-Diisopropylethylamine, DMF = dimethylformamide, EDC = 1-Ethyl-3-(3-dimethylaminopropyl)carbodiimide, FK228 = Romidepsin, GAPDH = glyceraldehyde 3-phosphate dehydrogenase, HBI-8000 = Chidamide, HDAC = histone deacetylase, HOBt = 1-hydroxybenzotriazole, Hz = Hertz, IC₅₀ = half maximal inhibitory concentration, J = coupling constants, LBH589 = Panobinostat, MPLC = medium pressure liquid chromatography, NMR = nuclear magnetic resonance, PXD101 = Belinostat, SAHA = Vorinostat, ZBG = zinc-binding group, Zn²⁺ = zinc ion.

Keywords: drug design, histone deacetylases, salicylamide, small molecule, zinc-binding group

Editor: Chang Chen.

This research was supported by Basic Science Research Program through the National Research Foundation of Korea (NRF) funded by the Ministry of Education (NRF-2016R1A6A1A03011325 and 2016R1D1A1B01009559).

Availability of data and materials: All data generated or analyzed in this study are included in this published article.

Ethics approval and consent to participate: Not applicable.

Patient consent for publication: Not applicable.

The authors declare that they have no competing interests.

The authors have no conflicts of interest to disclose.

Supplemental Digital Content is available for this article.

All data generated or analyzed during this study are included in this published article [and its supplementary information files];

College of Pharmacy, Keimyung University, Daegu, Republic of Korea.

* Correspondence: Young Ho Seo, Keimyung University, Daegu, Republic of Korea (e-mail: seoyho@kmu.ac.kr).

Copyright © 2022 the Author(s). Published by Wolters Kluwer Health, Inc. This is an open access article distributed under the terms of the Creative Commons Attribution-Non Commercial License 4.0 (CCBY-NC), where it is permissible to download, share, remix, transform, and buildup the work provided it is properly cited. The work cannot be used commercially without permission from the journal.

How to cite this article: Kim JH, Ali KH, Oh YJ, Seo YH. Design, synthesis, and biological evaluation of histone deacetylase inhibitor with novel salicylamide zinc binding group. *Medicine* 2022;101:17(e29049).

Received: 1 September 2021 / Received in final form: 28 November 2021 / Accepted: 11 December 2021

<http://dx.doi.org/10.1097/MD.00000000000029049>

1. Introduction

Lysine acetylation is a reversible post-translational modification regulated by histone deacetylases (HDACs) and their counterpart histone acetyltransferases.^[1,2] This post-translational modification plays an important role in regulating gene transcription and protein function. Histone deacetylases (HDACs) require a zinc ion (Zn²⁺) to catalyze the cleavage of acetyl groups from ϵ -N-acetyl-lysine side chains of histone and non-histone proteins.^[3] The zinc-dependent HDACs are divided into 4 classes, including class I (HDAC 1, 2, 3, and 8), class IIa (HDAC 4, 5, 7, and 9), class IIb (HDAC6 and 10), and class IV (HDAC11). Over the past decade, HDACs have emerged as important drug targets with a broad range of applications, such as treating cancers and central nervous system diseases.^[4–9] To date, 5 HDAC inhibitors are globally approved (Fig. 1). Four HDAC inhibitors, including Vorinostat (SAHA), Romidepsin (FK228), Belinostat (PXD101), and Panobinostat (LBH589), are approved by the United States Food and Drug Administration for the treatment of cutaneous T-cell lymphoma and multiple myeloma, and Chidamide (HBI-8000) is approved by the Chinese Food and Drug Administration for the treatment of cutaneous T-cell lymphoma.^[10–14]

A majority of HDAC inhibitors share a common pharmacophore, consisting of 3 distinct groups: a capping group, a linker group, and a zinc-binding group (ZBG), as shown in Fig. 2.^[15–17] The capping group binds to the external surface area of the active site pocket, the linker group connects the ZBG and the cap, and

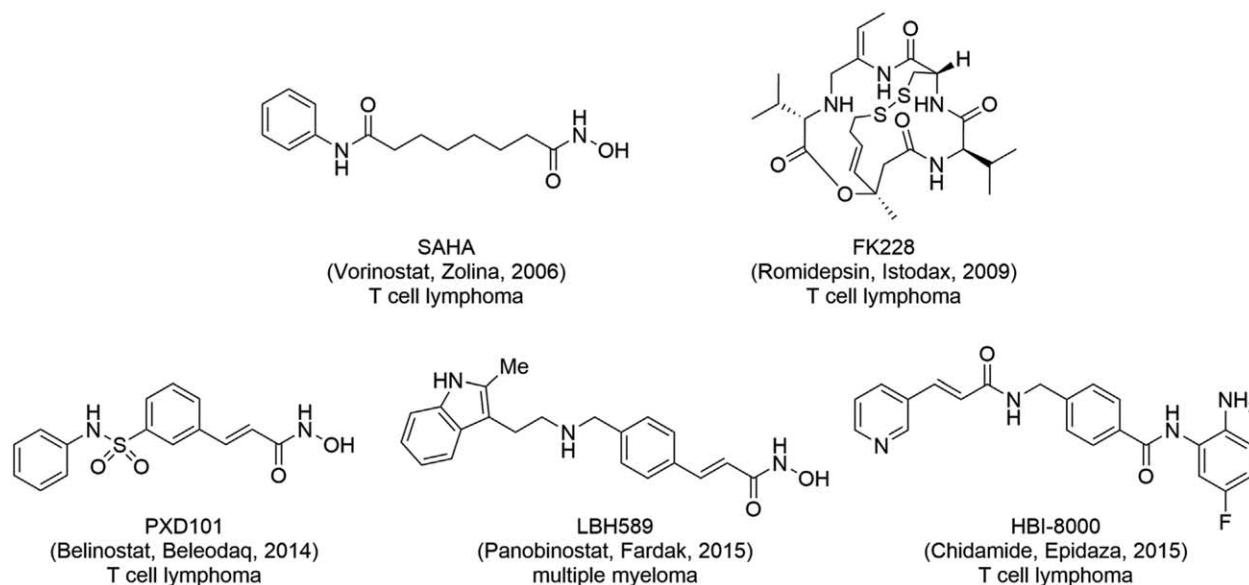


Figure 1. Structures of FDA-approved HDAC inhibitors. FDA=Food and Drug Administration, HDAC=histone deacetylase.

the ZBG chelates the catalytic zinc ion in the active site, which is critical for the catalytic function of HDAC enzymes. Despite the importance of ZBGs in potency and isoform selectivity, a relatively small number of studies on ZBGs have been conducted. Moreover, the most commonly used ZBG, hydroxamic acid, has limitations of poor pharmacokinetics and nonspecific metal-binding properties, highlighting its limitations in clinical use.^[18,19] Therefore, there is growing interest in finding novel ZBGs for the development of HDAC inhibitors.

To address the need for novel ZBGs, we explored salicylic acid as a potential novel ZBG. Salicylic acid is a natural compound, commonly obtained from the willow tree bark and responsible for the anti-inflammatory effects of aspirin.^[20] More importantly, a number of studies have indicated that salicylic acid and its

derivatives can chelate zinc ions in a bidentate fashion due to the existence of the hydroxyl group (–OH) in the ortho position to the carbonyl group (C=O).^[21–23] Based on the zinc chelating property of the salicylate structure, we decided to design a new HDAC inhibitor (5) by replacing the hydroxamic acid ZBG of SAHA with a salicylamide group, as illustrated in Fig. 2.

2. Materials and methods

2.1. General synthesis methods

All reagents and solvents were purchased from commercial suppliers and were used without further purification. Experiments involving moisture-sensitive substances were performed under inert atmosphere using argon and rotary evaporator was employed to evaporative and concentrating purposes. Analytical thin-layer chromatography (TLC), Supplemental Digital Content, <http://links.lww.com/MD2/A944> was performed on pre-coated silica gel F₂₅₄ TLC plates (E, Merck) which were visualized under UV lamp (254 nm) or iodine staining. Column chromatography was conducted with the help of hexane/ethyl acetate phase under medium pressure on silica (Merck Silica Gel 40–63 m) or performed by medium pressure liquid chromatography (MPLC, Supplemental Digital Content, <http://links.lww.com/MD2/A943> Biotage Isolera One instrument equipped with 254 and 280 nm UV detector) using silica gel cartridges (Biotage SNAP HP-Sil). Nuclear magnetic resonance (NMR; Supplemental Digital Content, <http://links.lww.com/MD2/A946>) analyses were carried out using a JNM-ECZ500R (500 MHz) instrument manufactured by JEOL Ltd. Chemical shifts are reported in parts per million (δ). The deuterium lock signal of the sample solvent was used as a reference, and coupling constants (*J*) were given in hertz (Hz). The splitting pattern abbreviations are as follows: s, singlet; d, doublet; t, triplet; q, quartet; dd, doublet of doublet; td, triplet of doublet; m, multiplet. The purity of final compound was confirmed to be higher than 95% by analytical high performance liquid chromatography performed with a dual pump Shimadzu LC-6AD system equipped with a VP-ODS C18 column (4.6 × 250 mm, 5 μ m,

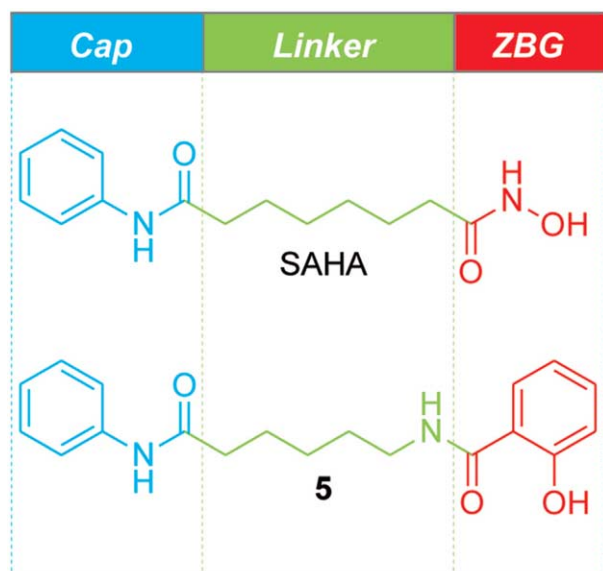


Figure 2. Drug design with a novel zinc binding group (ZBG).

Shimadzu). Mass spectrometric analysis was performed using an Agilent 6530 Accurate-Mass Quadrupole Time-of-Flight Liquid Chromatography/Mass Spectrometry, Supplemental Digital Content, <http://links.lww.com/MD2/A945> system with an Agilent 1290 Infinity LC (Agilent Technologies, Santa Clara, CA).

2.2. Synthetic scheme

The synthesis of the target compound 5 is illustrated in Scheme 1. We first commenced the synthesis of compound 2 following the previously reported procedure with a slight modification.^[24,25] Briefly, the protection reaction of commercially purchased 6-aminohexanoic acid (1) with di-*tert*-butyl dicarbonate (Boc₂O) in the presence of sodium hydroxide quantitatively provided compound 2. We then carried out an 1-Ethyl-3-(3-dimethylamino-propyl)carbodiimide (EDC)-mediated amide coupling reaction of compound 2 with aniline in the presence of *N,N*-Diisopropylethylamine (DIPEA) and 1-hydroxybenzotriazole (HOBT), successfully furnishing compound 3 in 23% yield. Subsequently, acidic cleavage of the *N*-Boc protecting group provided compound 4 in a quantitative yield. Finally, the amide coupling reaction of compound 4 with salicylic acid afforded the target compound 5 in 48% yield.

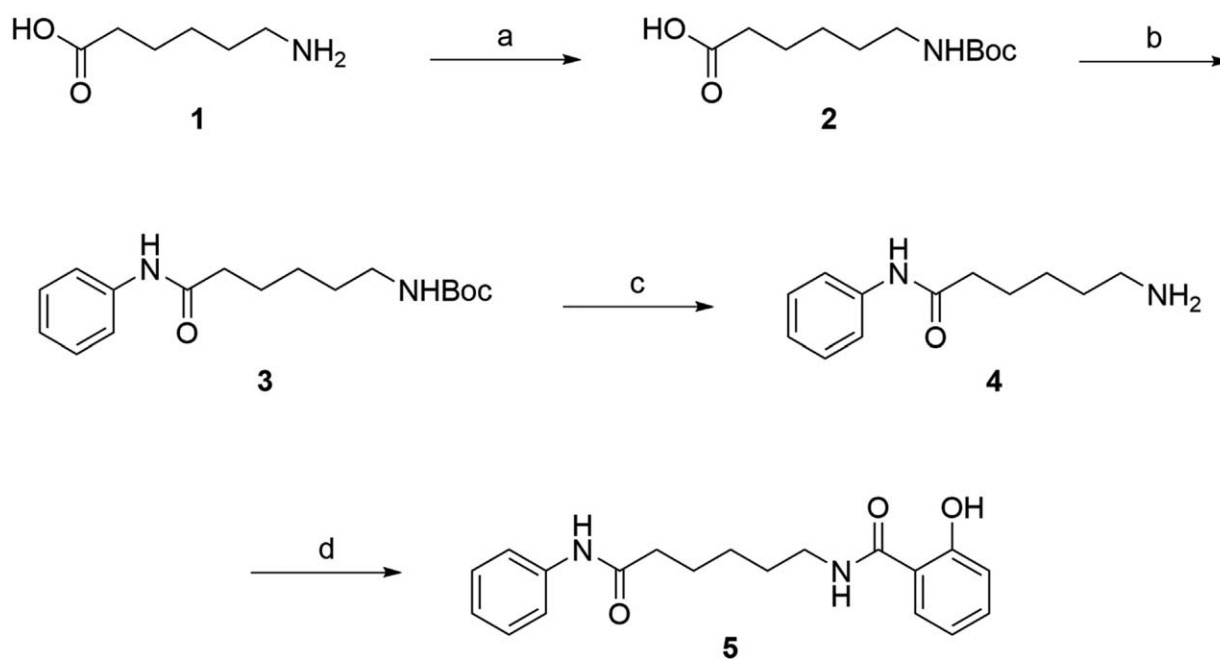
6-((*tert*-Butoxycarbonyl)amino)hexanoic acid (2) Commercially purchased 6-aminohexanoic acid (1.01g, 7.62 mmol) was dissolved in a mixture of dioxane (110 mL) and water (55 mL) to which 1 M aqueous solution of NaOH (10 mL, 7.62 mmol) was added. This was followed by introduction of Boc₂O (1.83 g, 8.39 mmol) at 0°C. The reaction mixture was allowed to stir at room temperature for 3 hours after which the mixture was concentrated under reduced pressure using a rotary evaporator. The aqueous solution was then washed with ethyl acetate (50 mL) and the pH was lowered to 1 using 1N aqueous HCl. Following that the aqueous layer was extracted with ethyl acetate (3 × 50 mL). The combined organic phase was dried over MgSO₄, filtered, and concentrated under reduced pressure to get compound 2 in 100%

yield which was used in the next step without further purification. ¹H-NMR (500 MHz, DMSO-d₆) δ 11.97 (s, 1H), 6.75 (t, *J*=5.4 Hz, 1H), 2.87 (q, *J*=6.7 Hz, 2H), 2.17 (t, *J*=7.4 Hz, 2H), 1.43–1.47 (m, 4H), 1.34 (t, *J*=7.7 Hz, 9H), 1.18–1.24 (m, 2H).

tert-Butyl (6-oxo-6-(phenylamino)hexyl)carbamate (3) Compound 2 (0.70 g, 3.06 mmol), aniline (0.28 g, 3.06 mmol), EDC (0.52 g, 3.37 mmol), DIPEA (0.64 mL, 3.67 mmol), and HOBT (0.41 g, 3.06 mmol) were dissolved in dimethylformamide (DMF) (40 mL) and stirred at room temperature for 3 hours under argon. The reaction mixture was then concentrated under reduced pressure to remove excessive DMF, diluted with ethyl acetate (80 mL), and washed with 1N HCl (80 mL), followed by brine (80 mL). The organic layer was collected and dried over MgSO₄, concentrated under reduced pressure, and purified by MPLC (Biotage SNAP HP-Sil column) to afford compound 3 in 23% yield. *R*_f=0.26 (4:6 ethyl acetate/hexane). ¹H NMR (500 MHz, CDCl₃) δ 7.94 (s, 1H), 7.52 (d, *J*=8.0 Hz, 2H), 7.26 (t, *J*=7.7 Hz, 2H), 7.05 (t, *J*=7.4 Hz, 1H), 4.67 (s, 1H), 3.07 (q, *J*=6.3 Hz, 2H), 2.31 (t, *J*=7.7 Hz, 2H), 1.66–1.72 (m, 2H), 1.41–1.49 (m, 11H), 1.32 (td, *J*=15.2, 8.4 Hz, 2H).

6-Amino-*N*-phenylhexanamide (4) A mixture of compound 3 (0.071 g, 0.23 mmol) and 2N HCl in diethyl ether (5 mL) was stirred at room temperature for 24 hours. The reaction mixture was concentrated under reduced pressure to afford compound 4 in 100% yield which did not require any further purification. ¹H NMR (500 MHz, DMSO-d₆) δ 10.02 (s, 1H), 7.93 (s, 2H), 7.60 (d, *J*=8.0 Hz, 2H), 7.26 (t, *J*=7.7 Hz, 2H), 7.00 (t, *J*=7.4 Hz, 1H), 2.75 (q, *J*=6.9 Hz, 2H), 2.31 (t, *J*=7.4 Hz, 2H), 1.53–1.59 (m, 4H), 1.33 (q, *J*=7.8 Hz, 2H).

2-Hydroxy-*N*-(6-oxo-6-(phenylamino)hexyl)benzamide (5) Compound 4 (0.064 g, 0.31 mmol), salicylic acid (0.028 g, 0.20 mmol), EDC (0.062 g, 0.40 mmol), HOBT (0.027 g, 0.20 mmol), and DIPEA (0.040 mL, 0.22 mmol) were taken together and dissolved in DMF (20 mL). The reaction mixture was then allowed to stir at room temperature for 12 hours under argon.



Scheme 1. Synthesis of compound 5. Reagents and conditions: (A) Boc₂O, dioxane, 1 M NaOH, rt, 12 hours, 100% (B) aniline, EDC, DIPEA, HOBT, DMF, rt, 12 hours, 23% (C) HCl, diethyl ether, rt, 24 hours, 100% (D) salicylic acid, EDC, DIPEA, HOBT, DMF, rt, 12 hours, 48%.

Upon completion, the mixture was diluted with ethyl acetate (100 mL) and washed with water (100 mL). The organic layer was washed twice with 1N HCl (100 mL), followed by brine (100 mL), dried over Na₂SO₄, concentrated under reduced pressure, and purified by MPLC (Biotage SNAP HP-Sil column) to obtain compound 5 in 48% yield. $R_f=0.42$ (5:5 ethyl acetate/hexane). ¹H NMR (500 MHz, CD₃OD) δ 7.71–7.73 (m, 1H), 7.50–7.52 (m, 2H), 7.35 (td, $J=7.7, 1.5$ Hz, 1H), 7.27 (t, $J=8.0$ Hz, 2H), 7.10–7.02 (1H), 6.90–6.81 (2H), 3.39 (t, $J=7.2$ Hz, 2H), 2.38 (t, $J=7.4$ Hz, 2H), 1.72–1.78 (m, 2H), 1.64–1.70 (m, 2H), 1.43–1.49 (m, 2H). ¹³C NMR (126 MHz, CD₃OD) δ 174.53, 170.96, 161.23, 139.83, 134.64, 129.74, 128.70, 125.13, 121.31, 120.01, 118.43, 116.99, 40.29, 37.80, 30.19, 27.61, 26.55. ESI MS (m/z) = 327.05 [M + H]⁺.

2.3. Docking study

In silico docking of compound 5 with the 3D coordinates of the X-ray crystal structures of HDAC2 (PDB code: 4LXZ) was accomplished using the AutoDock program downloaded from the Molecular Graphics Laboratory of the Scripps Research Institute. The reason behind choosing AutoDock was the ability of this program to use genetic algorithm and generate the ligand poses inside a known or predicted binding site through the Lamarckian version of the genetic algorithm, where the changes in conformations adopted by molecules after in situ optimization are used as subsequent poses for the offspring. In the docking experiments, Gasteiger charges were placed on the X-ray structures of HDAC2 with compound 5, using tools from the AutoDock suite. A grid box centered on the substrate-binding pocket of the HDAC2 enzyme with 50 × 50 × 50 points and 0.375 Å spacing was selected for the ligand during docking experiments. Among the docking parameters population size was set to 150, the number of generations to 27,000, the number of evaluations to 2,500,000, and the number of docking runs were adjusted to 100 with a cutoff of 1 Å for the root-mean-square tolerance for the grouping of each docking run. Rendering of the pictures was generated with the help of PyMol (DeLano Scientific).

2.4. Biology materials

Dulbecco's modified Eagle's medium (DMEM) with L-glutamine was purchased from GenDEPOT (Barker, TX), fetal bovine serum was purchased from HyClone, and penicillin and streptomycin were purchased from Gibco BRL (Gaithersburg, MD). Antibodies for α -tubulin, Ac- α -tubulin (Lys40), Histone H3, Ac-Histone H3 (Lys9), HDAC1, HDAC6, and glyceraldehyde 3-phosphate dehydrogenase (GAPDH) were purchased from Cell Signaling Technology (Boston, MA). Goat anti-rabbit IgG horseradish peroxidase conjugate was purchased from Santa Cruz Biotechnology (Santa Cruz, CA). Cell Titer 96 Aqueous One Solution cell proliferation assay kit was purchased from Promega (Madison, WI). Amersham ECL Select western blotting Detection Reagent was purchased from GE Healthcare. HDAC fluorogenic assay kits (HDAC1, #50061; HDAC2, #50062; HDAC3, #50073; HDAC4, #50064; HDAC6, #50076; HDAC11, #50687) were bought from BPS Bioscience (San Diego, CA).

2.5. Cell culture

MDA-MB-231 breast cancer cells were grown in Dulbecco's modified Eagle's medium with L-glutamine supplemented with

10% fetal bovine serum, 100 units/mL penicillin, and 10 mg/mL streptomycin. The cells were incubated in a humidified atmosphere (37°C, 5% CO₂).

2.6. HDAC assay

The enzymatic HDAC assay was performed according to the manufacturer's protocol (BPS Bioscience). Briefly, HDAC assay buffer (35 μ L) was mixed with 5 μ L of bovine serum albumin (1 mg/mL) and 5 μ L of HDAC substrate (200 mM) in a 96-well black plate. The HDAC enzyme (5 μ L, 7 ng/mL) was added to each well, treated with various concentrations of compound 5 (5 μ L) or SAHA (5 μ L) as a positive control, and then incubated at 37°C for 30 minutes. Upon completion of the incubation period, 50 μ L of undiluted HDAC developer was added to each well, and the plate was incubated at room temperature for 15 minutes. Fluorescence intensity was measured using a Tecan Infinite F200 Pro plate reader at the excitation and emission wavelengths of 360 and 460 nm respectively. The half maximal inhibitory concentration (IC₅₀) values and curve fits were obtained using Prism software (GraphPad Software).

2.7. Cell proliferation assays

MDA-MB-231 cells (2×10^3 cells/well) were seeded in a transparent 96-well plate, to which the medium volume was made up to 100 μ L per well, and the cells were allowed to attach overnight. Various concentrations of compound 5 were added to the wells, and the cells were incubated at 37°C for 1, 2, and 3 days. Cell viability was determined using the Promega Cell Titer 96 Aqueous One Solution cell proliferation assay. The absorbance values were recorded at 490 nm with a 96-well plate reader, and presented as a percentage of absorbance from cells incubated in DMSO alone.

2.8. Western blot

MDA-MB-231 cells were seeded in 100 mm culture dishes, incubated overnight, and treated with the indicated concentrations of compound 5 for 24 hours. The cells were then harvested and lysed on ice using Radio-Immunoprecipitation Assay buffer (23 mM Tris-HCl pH 7.6, 130 mM NaCl, 1% NP-40, 1% sodium deoxycholate, 0.1% SDS) supplemented with protease and phosphatase inhibitor cocktails. Next, 30 μ g of protein per lane was separated using sodium dodecyl sulphate-polyacrylamide gel electrophoresis (SDS-PAGE) and transferred to a polyvinylidene fluoride membrane (Bio-Rad, Hercules, CA). The membrane was blocked with 5% skim milk in Tris buffered saline with Tween and then incubated with the corresponding primary antibodies (α -tubulin, Ac- α -tubulin, Histone H3, Ac-Histone H3, HDAC1, HDAC6, or GAPDH) overnight. This was followed by the treatment with an appropriate secondary antibody (Santa Cruz, CA) coupled to horseradish peroxidase. The resulting membranes blotted with proteins were visualized using ECL chemiluminescence according to the manufacturer's instructions (GE Healthcare, USA).

2.9. Assessment of cell morphology

MDA-MB-231 cells (1×10^4 cells/well) were seeded into a 6-well plate. After 24 hours, the culture medium was replaced with fresh medium containing compound 5 and further incubated for

Table 1
In vitro inhibitory activity of compound 5 against histone deacetylase isotypes.

| HDAC [*] subtype | | Compound 5 (IC ₅₀ ; μM) | SAHA [†] (IC ₅₀ ; μM) |
|---------------------------|--------|------------------------------------|---|
| Class I | HDAC1 | 22.2 ± 2.69 | 0.14 ± 0.02 |
| | HDAC2 | 27.3 ± 3.71 | 0.44 ± 0.01 |
| | HDAC3 | 7.9 ± 2.57 | 0.73 ± 0.03 |
| Class IIa | HDAC4 | >100 | 5.40 ± 2.5 |
| Class IIb | HDAC6 | >100 | 0.03 ± 0.01 |
| Class IV | HDAC11 | >100 | >100 |

Data are presented as the mean ± SD (n=2).

^{*}HDAC=histone deacetylase.

[†]SAHA=vorinostat.

24 hours. Cell morphology was observed using a light microscope at 200× magnification.

2.10. Statistical analysis

The results were quantified using data from multiple individual experiments (n) and presented as mean ± standard deviation. The assessment of *P*-value was carried out using Student *t* test and the statistical significance was considered as **P* < .05, ***P* < .01, ****P* < .001.

3. Results

3.1. Compound 5 inhibits class I HDAC enzymes

Upon synthesis completion, we examined the inhibitory activity of compound 5 to HDAC isoforms, using FDA-approved HDAC inhibitor SAHA as a reference drug. As shown in Table 1, compound 5 could inhibit class I HDAC isoforms, including HDAC1, 2, and 3 (HDAC1 IC₅₀=22.2 μM, HDAC2 IC₅₀=27.3 μM, and HDAC3 IC₅₀=7.9 μM), but failed to inhibit other HDAC classes, including class IIa, IIb, and IV. In contrast, the pan-HDAC inhibitor, SAHA, efficiently inhibited HDAC 1, 2, 3, and 6 at submicromolar concentrations (HDAC1 IC₅₀=0.14 μM, HDAC2 IC₅₀=0.44 μM, HDAC3 IC₅₀=0.73 μM, and HDAC6 IC₅₀=0.03 μM). SAHA also exhibited mediocre

inhibitory activity against class IIa HDAC4 (IC₅₀=5.40 μM) and no inhibition against class IV HDAC11 up to 100 μM concentration, which are in line with the previously reported data.^[26,27] Despite its relatively mediocre inhibitory activity, the salicylamide moiety of compound 5 could act as a ZBG with a modest selectivity for class I HDACs in the development of HDAC inhibitors.

3.2. In vitro anti-proliferative activity of compound 5 against MDA-MB-231 cells

Furthermore, we investigated the dose- and time-dependent effect of compound 5 on the cell viability of human breast carcinoma MDA-MB-231 cells. MDA-MB-231 cells were treated with various concentrations of compound 5 for 1, 2, and 3 days, and cell viability was measured using MTS colorimetric assay (Fig. 3). The assay indicated that compound 5 exhibited no anti-proliferative activity against MDA-MB-231 cells up to 100 μM concentration. However, compound 5 displayed mediocre dose- and time-dependent anti-proliferative activity at concentrations from 300 to 1000 μM. The treatment of cells with compound 5 (500 and 1000 μM) for 3 days impaired 64% and 81% of MDA-MB-231 cell growth, respectively. This relatively poor cellular anti-proliferative activity was probably due to the higher IC₅₀ value of compound 5 in the HDAC enzyme assay, shown in Table 1.

We further studied the underlying cellular mechanisms and dose-response of compound 5 (Fig. 4). Accordingly, we treated MDA-MB-231 cells with compound 5 at concentrations ranging from 50 to 500 μM for 24 hours and analyzed the levels of Histone H3, acetylated Histone H3, α-tubulin, acetylated α-tubulin, HDAC1, and HDAC6 using western blot. Histone H3 is a substrate of HDAC1, and α-tubulin is a substrate of the HDAC6 enzyme. Therefore, the inhibition of HDAC1 and HDAC6 epigenetically induces the acetylation of Histone H3 and α-tubulin, respectively. As shown in Fig. 4, compound 5 dose-dependently increased the acetylation of Histone H3 via the inhibition of HDAC1 enzyme up to 300 μM concentration. In contrast, compound 5 promoted the acetylation of α-tubulin at concentrations ranging from 300 to 500 μM. Interestingly, compound 5 decreased the expression level of HDAC6 in a dose-

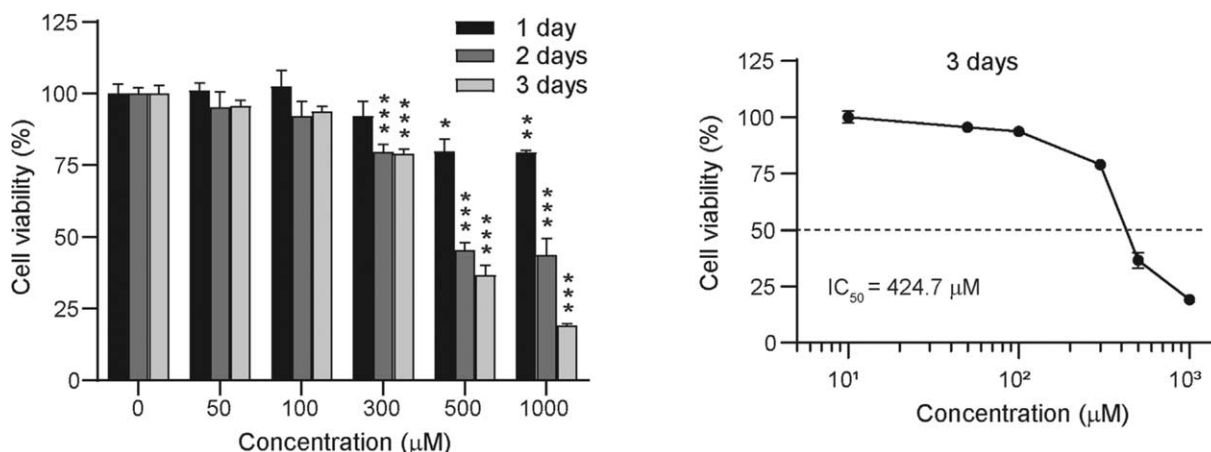


Figure 3. Dose- and time-dependent effect of compound 5 on the cell viability of human breast carcinoma MDA-MB-231 cells. Data are presented as mean ± SD (n=4). The results were considered statistically significant **P* < .05, ***P* < .01, ****P* < .001.

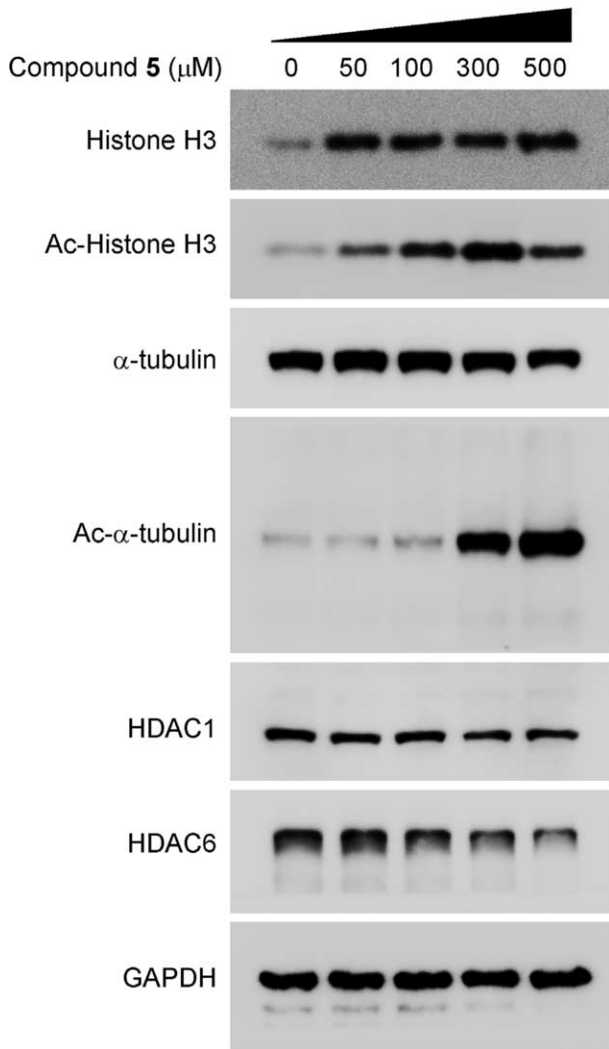


Figure 4. Effect of compound 5 on the acetylation status of Histone H3 and α -tubulin. MDA-MB-231 cells were incubated with the indicated concentrations of compound 5 for 24 hours and the expression level of Histone H3, Ac-Histone H3, α -tubulin, Ac- α -tubulin, HDAC1, HDAC6, and GAPDH were analyzed using Western blotting. DMSO (D) was used as a negative control. GAPDH=glyceraldehyde 3-phosphate dehydrogenase, HDAC=Histone deacetylase.

dependent manner, and the administration of compound 5 at 500 μ M concentration significantly depleted the expression level of HDAC6, in that the expression level of internal standard, GAPDH remained unchanged. This result suggested that compound 5 promoted the acetylation of α -tubulin via the downregulation of HDAC6 rather than the inhibition of HDAC6 enzyme activity. The western blotting experiment indicated that compound 5 selectively inhibited HDAC1 over HDAC6, which was well correlated with the results in HDAC enzyme assay, shown in Table 1.

3.3. Compound 5 induces morphological changes in MDA-MB-231 cells

Microtubules are highly dynamic biological polymers composed of tubulin subunits that play an essential role in cell division, cell migration, and cytoplasm architecture. Recent studies have demonstrated that the acetylation of α -tubulin leads to the stabilization of microtubules, highlighting the importance of tubulin acetylation in the dynamic microtubule assembly.^[28] Hence, we examined the effect of compound 5 on the morphology of MDA-MB-231 cells (Fig. 5). The treatment of MDA-MB-231 cells with compound 5 induced morphological changes in cells in a dose-dependent manner. As concentration increased, MDA-MB-231 cells became more elongated and spindle-shaped. These morphological changes were most significant at concentrations from 300 to 500 μ M. This observation indicated that the acetylation of α -tubulin at concentrations ranging from 300 to 500 μ M stabilized microtubules, resulting in elongated and spindle-shaped morphology changes.

3.4. Molecular docking study of compound 5

Recently, the need to predict and understand the binding mode of protein and ligand has become quite popular in the field of drug discovery. Our interest in this domain led us to assess the binding mode of compound 5 in the binding pocket of HDAC2. The crystal structure of HDAC2 (PDB code: 4LXZ) was used in this study. As shown in Fig. 6, the docking simulation of compound 5 showed a similar interaction pattern to the crystal structure of HDAC2-SAHA complex. A new ZBG, the salicylamide of compound 5, was positioned at the bottom of the binding pocket and the C=O, and the phenolic oxygen (OH) of salicylamide coordinated the active Zn^{2+} ion in a bidentate

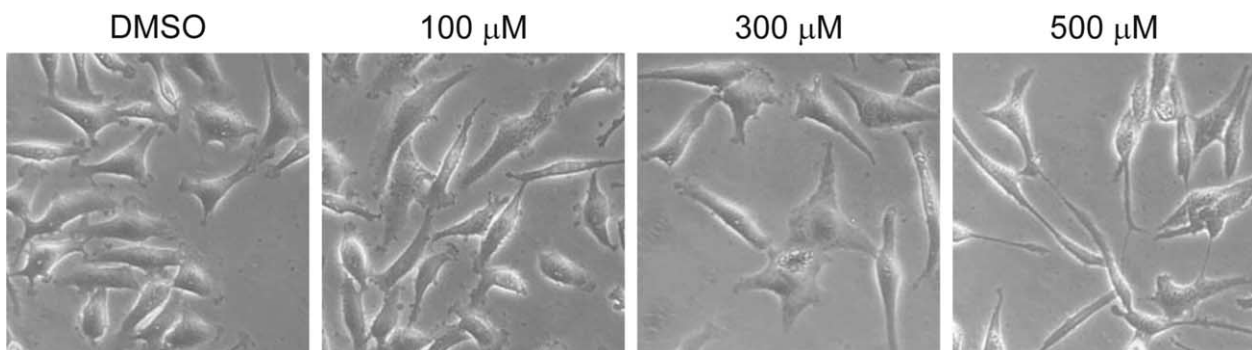


Figure 5. Effect of compound 5 on the cell morphology of MDA-MB-231 cells. MDA-MB-231 cells were treated with the indicated concentrations of compound 5 for 24 hours and cell images were taken at 200 \times magnification.

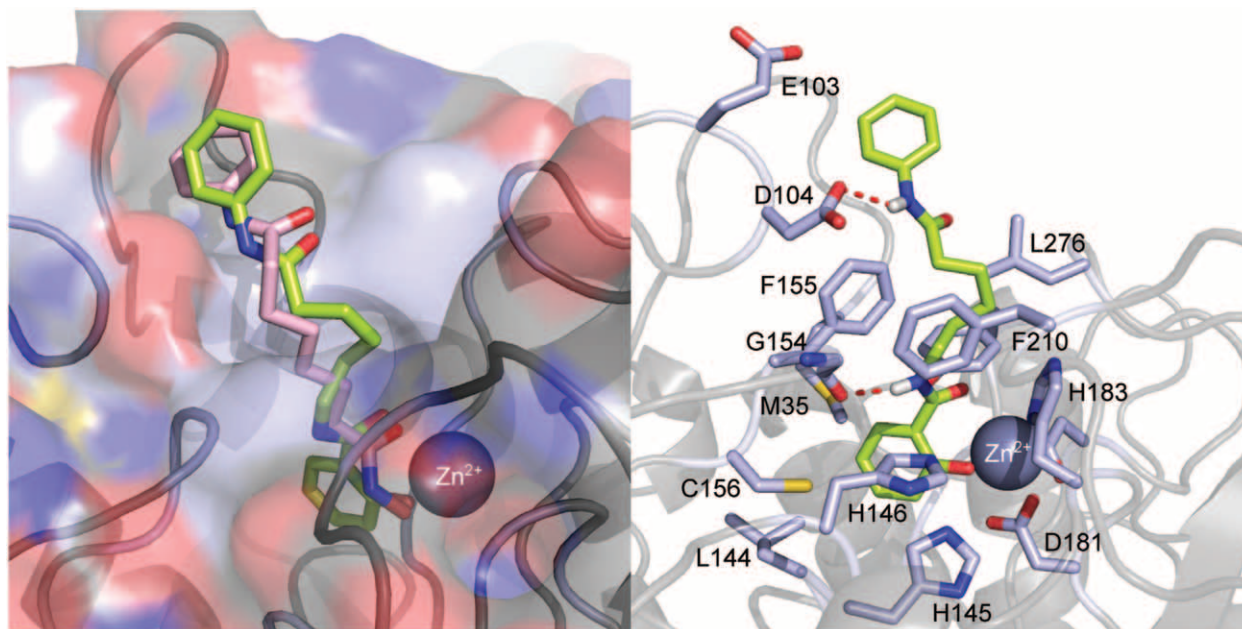


Figure 6. Molecular docking pose of compound 5 bound in the substrate-binding pocket of HDAC2 (PDB code: 4LXZ). The docking pose of compound 5 (lime) and the crystal structure of SAHA (pink) complex were overlapped in the substrate-binding pocket of HDAC2. The oxygen, nitrogen, and hydrogen atoms of compound 5 and SAHA are shown in red, blue, and white, respectively. The side chains of the binding site are colored according to the atom types (carbon, light blue; oxygen, red; nitrogen, blue) and labeled with their residue name. The hydrogen bonds are shown as dashed red lines. The docking poses are visualized using PyMOL1.3.

fashion. The phenyl ring of salicylamide occupied the very bottom of the substrate binding pocket, forming a proximal van der Waals interaction with side chains of Leu144, Cys156, and Met35. The middle alkyl chain of compound 5 fit into the hydrophobic channel and formed a hydrophobic interaction with the side chains of Phe155, Phe210, and Leu276 residues. The terminal anilide (Cap group) occupied the surface outside of the substrate binding pocket, while the C=O of the anilide formed a hydrogen bond with Asp104 residue. Collectively, the docking study indicated that compound 5 could bind to the substrate binding pocket of HDAC2 with diverse intermolecular interactions.

4. Discussion

The use of salicylamide moiety as a ZBG in this study suggests the possibility of developing a new class of HDAC inhibitors that, in near future, could possibly be free from most of the undesired side effects that currently available hydroxamic acid based HDAC inhibitors present. Due to close resemblance of compound 5 with the FDA approved HDAC inhibitor SAHA, SAHA was used as a reference drug in experiments. A decrease in the HDAC enzyme inhibitory activity upon compromising the typical hydroxamic group and using salicylamide instead is understandable and consistent with the finding from the recent studies.^[29,30] Despite interacting with the active Zn^{2+} ion of HDAC pocket in a bidentate manner, that is similar to the case of most hydroxamic acids including SAHA, the aforementioned decline in inhibitory activity might be attributed to the bulky nature of salicylamide. A modest selectivity for class I HDACs (HDAC1, 2, and 3) over other HDAC classes (HDAC4, 6, and 11) in the HDAC enzyme assay indicates that along with cap and linker, ZBG also has an influence upon this phenomenon.

Although the anti-proliferative potential of the compound 5 appears to be mediocre, the impairment in the growth of a triple negative human breast carcinoma (MDA-MB-231 cells) in a dose- and time-dependent manner is encouraging but definitely needs further optimization. It is also noteworthy that MDA-MB-231 cells upon treatment with compound 5 induced the acetylation of histone H3 more efficiently as compared with α -tubulin suggesting that compound 5 is a class I selective HDAC inhibitor. Moreover, it is important to note that the compound 5 caused a visually distinguishable change in the morphology of MDA-MB-231 cells at concentrations of 300 μ M and above which further supports the argument about the promise that salicylamide shows as a new ZBG option for future HDAC inhibitors. A shift from oval to an elongated appearance with increasing concentrations of compound 5 (Fig. 4) hints towards a reduced invasive behavior and retardation of cell viability.^[31]

5. Conclusion

To the best of our knowledge, this is the first report of an HDAC inhibitor with a salicylamide ZBG, furnishing class I HDAC selectivity. This new finding warrants further studies on hit-to-lead and lead optimization of salicylamide ZBG, and these studies will be reported in due course.

Author contributions

Young Ho Seo conceived and designed the study. Ji Hyun Kim, Khan Hashim Ali, Yong Jin Oh, and Young Ho Seo performed the experiments, analyzed the data, and wrote the manuscript. All authors read and approved the final manuscript and agreed to be accountable for all aspects of the research.

Conceptualization: Young Ho Seo.

Funding acquisition: Young Ho Seo.

Methodology: Young Ho Seo, Ji Hyun Kim, Khan Hashim Ali, Yong Jin Oh.

Project administration: Young Ho Seo.

Resources: Young Ho Seo.

Supervision: Young Ho Seo.

Writing – review & editing: Young Ho Seo, Khan Hashim Ali, Yong Jin Oh.

Data curation: Ji Hyun Kim.

Investigation: Ji Hyun Kim, Khan Hashim Ali, Yong Jin Oh.

Software: Ji Hyun Kim, Khan Hashim Ali, Yong Jin Oh.

Writing – original draft: Ji Hyun Kim, Khan Hashim Ali.

References

- [1] Drazic A, Myklebust LM, Ree R, Arnesen T. The world of protein acetylation. *Biochim Biophys Acta* 2016;1864:1372–401.
- [2] Glozak MA, Sengupta N, Zhang X, Seto E. Acetylation and deacetylation of non-histone proteins. *Gene* 2005;363:15–23.
- [3] Seto E, Yoshida M. Erasers of histone acetylation: the histone deacetylase enzymes. *Cold Spring Harb Perspect Biol* 2014;6:a018713.
- [4] Lim J, Song Y, Jang JH, et al. Aspirin-inspired acetyl-donating HDACs inhibitors. *Arch Pharm Res* 2018;41:967–76.
- [5] Seo SY. Multi-targeted hybrids based on HDAC inhibitors for anti-cancer drug discovery. *Arch Pharm Res* 2012;35:197–200.
- [6] Choi MA, Park SY, Chae HY, Song Y, Sharma C, Seo YH. Design, synthesis and biological evaluation of a series of CNS penetrant HDAC inhibitors structurally derived from amyloid-beta probes. *Sci Rep* 2019;9:13187.
- [7] Sharma C, Oh YJ, Park B, et al. Development of thiazolidinedione-based HDAC6 inhibitors to overcome methamphetamine addiction. *Int J Mol Sci* 2019;20:
- [8] Yu N, Chen P, Wang Q, et al. Histone deacetylase inhibitors differentially regulate c-Myc expression in retinoblastoma cells. *Oncol Lett* 2020;19:460–8.
- [9] Bobrowicz M, Slusarczyk A, Domagala J, et al. Selective inhibition of HDAC6 sensitizes cutaneous T-cell lymphoma to PI3K inhibitors. *Oncol Lett* 2020;20:533–40.
- [10] Duvic M, Talpur R, Ni X, et al. Phase 2 trial of oral vorinostat (suberoylanilide hydroxamic acid, SAHA) for refractory cutaneous T-cell lymphoma (CTCL). *Blood* 2007;109:31–9.
- [11] Lee HZ, Kwitkowski VE, Del Valle PL, et al. FDA approval: Belinostat for the treatment of patients with relapsed or refractory peripheral T-cell lymphoma. *Clin Cancer Res* 2015;21:2666–70.
- [12] Lu X, Ning Z, Li Z, Cao H, Wang X. Development of chidamide for peripheral T-cell lymphoma, the first orphan drug approved in China. *Intractable Rare Dis Res* 2016;5:185–91.
- [13] Raedler LA. Farydak (Panobinostat): first HDAC inhibitor approved for patients with relapsed multiple myeloma. *Am Health Drug Benefits* 2016;9:84–7.
- [14] VanderMolen KM, McCulloch W, Pearce CJ, Oberlies NH. Romidepsin (Istodax, NSC 630176, FR901228, FK228, depsipeptide): a natural product recently approved for cutaneous T-cell lymphoma. *J Antibiot (Tokyo)* 2011;64:525–31.
- [15] Ling Y, Guo J, Yang Q, et al. Development of novel beta-carboline-based hydroxamate derivatives as HDAC inhibitors with antiproliferative and antimetastatic activities in human cancer cells. *Eur J Med Chem* 2018;144:398–409.
- [16] Li X, Zhang Y, Jiang Y, et al. Selective HDAC inhibitors with potent oral activity against leukemia and colorectal cancer: design, structure-activity relationship and anti-tumor activity study. *Eur J Med Chem* 2017;134:185–206.
- [17] Mehdiratta S, Wang RS, Huang HL, et al. 4-Indolyl-N-hydroxyphenylacrylamides as potent HDAC class I and IIB inhibitors in vitro and in vivo. *Eur J Med Chem* 2017;134:13–23.
- [18] Summers JB, Gunn BP, Mazdiyasi H, et al. In vivo characterization of hydroxamic acid inhibitors of 5-lipoxygenase. *J Med Chem* 1987;30:2121–6.
- [19] Kelly WK, Richon VM, O'Connor O, et al. Phase I clinical trial of histone deacetylase inhibitor: suberoylanilide hydroxamic acid administered intravenously. *Clin Cancer Res* 2003;9(10 pt 1):3578–88.
- [20] Wood JN. From plant extract to molecular panacea: a commentary on Stone (1763) 'An account of the success of the bark of the willow in the cure of the agues'. *Philos Trans R Soc Lond B Biol Sci* 2015;370:
- [21] Perrin DD. Stability of metal complexes with salicylic acid and related substances. *Nature* 1958;182:741–2.
- [22] An F, Gao B, Dai X, Wang M, Wang X. Efficient removal of heavy metal ions from aqueous solution using salicylic acid type chelate adsorbent. *J Hazard Mater* 2011;192:956–62.
- [23] Foye WO. Role of metal-binding in the biological activities of drugs. *J Pharm Sci* 1961;50:93–108.
- [24] Chen C, Yang X, Fang H, Hou X. Design, synthesis and preliminary bioactivity evaluations of 8-hydroxyquinoline derivatives as matrix metalloproteinase (MMP) inhibitors. *Eur J Med Chem* 2019;181:111563.
- [25] Huang C, Yin Q, Zhu W, et al. Highly selective fluorescent probe for vicinal-dithiol-containing proteins and in situ imaging in living cells. *Angew Chem Int Ed Engl* 2011;50:7551–6.
- [26] Yang Z, Shen M, Tang M, et al. Discovery of 1,2,4-oxadiazole-containing hydroxamic acid derivatives as histone deacetylase inhibitors potential application in cancer therapy. *Eur J Med Chem* 2019;178:116–30.
- [27] Song Y, Lim J, Seo YH. A novel class of anthraquinone-based HDAC6 inhibitors. *Eur J Med Chem* 2019;164:263–72.
- [28] Eshun-Wilson L, Zhang R, Portran D, et al. Effects of alpha-tubulin acetylation on microtubule structure and stability. *Proc Natl Acad Sci U S A* 2019;116:10366–71.
- [29] He J, Wang S, Liu X, et al. Synthesis and biological evaluation of HDAC inhibitors with a novel zinc binding Group. *Front Chem* 2020;8:
- [30] Li Y, Wang F, Chen X, et al. Zinc-dependent deacetylase (HDAC) inhibitors with different zinc binding groups. *Curr Top Med Chem* 2019;19:223–41.
- [31] Ziperstein MJ, Guzman A, Kaufman LJ. Breast cancer cell line aggregate morphology does not predict invasive capacity. *PLoS One* 2015;10: e0139523.